Published in final edited form as:
Med Image Comput Comput Assist Interv. 2012 ; 15(0 3): 123–130.

Unbiased groupwise registration of white matter tractography

Lauren J. O'Donnell[1,2,3], **William Wells III**[3], **Alexandra J. Golby**[2,3], and **Carl-Fredrik Westin**[1,3]

Lauren J. O'Donnell: odonnell@bwh.harvard.edu

[1]Laboratory for Mathematics in Imaging, BWH, Harvard Medical School, Boston MA USA

[2]Golby Lab, a Surgical Brain Mapping Laboratory, BWH, Harvard Medical School, Boston MA USA

[3]Surgical Planning Laboratory, BWH, Harvard Medical School, Boston MA USA

Abstract

We present what we believe to be the first investigation into unbiased multi-subject registration of whole brain diffusion tractography of the white matter. To our knowledge, this is also the first entropy-based objective function applied to fiber tract registration. To define the probability of fiber trajectories for the computation of entropy, we take advantage of a pairwise fiber distance used as the basis for a Gaussian-like kernel. By employing several values of the kernel's scale parameter, the method is inherently multi-scale. Results of experiments using synthetic and real datasets demonstrate the potential of the method for simultaneous joint registration of tractography.

Keywords

registration; white matter; tractography; diffusion MRI

1 Introduction

Automated medical or neuroscientific analyses of white matter tractography data, such as segmentation or labeling, creation of atlases, and measurement of tract statistics, all require initial alignment or normalization of tractography via some method. This alignment is most often performed by applying the transformations resulting from an image-based fractional anisotropy or diffusion tensor registration [18, 4]. However if the eventual goal is modeling and analysis of white matter tracts, it may be advantageous to register the tracts themselves, as the quantity being optimized during registration will be closely related to the final goal. In this work we explore the possibility of driving an unbiased multi-subject registration using the trajectory data produced by streamline tractography.

In contrast to the proposed approach, to our knowledge all other methods for simultaneous joint registration of tractography have been based on alignment of pre-defined fiber bundles. These methods have required a pre-existing tractography segmentation for each subject and have thus been limited to particular structures: corticospinal tract, forceps major, cingulum and inferior longitudinal fasciculus [1]; structures resulting from an initial clustering plus expert labels [19]; left uncinate and front-occipital fasciculi [17]; and the arcuate fasciculus, corticospinal tract, and middle cerebellar peduncles [3]. So far, methods that have performed registration using unlabeled fiber tracts from the whole brain, e.g. [9, 21, 12], have been limited to subject-to-subject (pairwise) registration.

In addition to tractography-based registration, our current work builds on two other categories of related work: fiber tract comparison, and groupwise image registration. Work in fiber tract clustering has led to many different metrics [16, 15, 10], generally based on distances computed between points along the tracts, often with conversion to fiber affinities using Gaussian kernels as in our proposed objective function. Tracts have also been analyzed via many styles of point-wise matching, for example [2, 12, 10, 1]. In the image registration field, several groups have proposed multiple-subject unbiased and template-based image registration methods. These include entropy-based congealing methods for 2D [8] and 3D [20] that find a population central tendency image by minimizing entropy, as well as methods that estimate a population template image that is the minimum distance (in the space of diffeomorphisms) from all input images [6, 4].

2 Methods

2.1 Objective function

Our basic approach is to represent a brain or atlas by a probability distribution on trajectories. A "brain" distribution is constructed as a kernel density estimate from the tractography, and an "atlas" distribution is constructed as a mixture of the constituent brain distributions. We then choose the alignment parameters on the collection of brains by maximizing the "sharpness" of the atlas, or minimizing its entropy.

Given a distance metric D between fibers we define the probability of a fiber f, given another fiber f_j, as

$$p(f|f_j)=\frac{1}{Z}e^{-\frac{D^2(f,f_j)}{\sigma^2}} \quad (1)$$

where the distance is used as the basis for a Gaussian-like kernel with standard deviation σ, and the normalization constant Z will be discussed later. Our current choice of D is discussed below, however this can in principle work for any of the many existing fiber distances from the literature. Next, the probability of a fiber f, given the set of all fibers A and their transformations T ("the atlas"), is defined as

$$p(f|A,T)=\frac{1}{|A|}\sum_j p(f|f_j \in A,T) \quad (2)$$

where all fibers f_j in A contribute to the total probability.

The Shannon entropy H of the distribution of fibers is the expected value of the negative log-probability of the fibers. In this case the set of current transformations T has been applied to the fibers (including the transformations T_i and T_j currently applied to fibers f_i and f_j), and we replace the expected value with the sample average value (using the weak law of large numbers).

$$H(f|A,T)=E(-log(p(f|A,T))) \quad (3)$$

$$=-\frac{1}{|A|}\sum_i log\frac{1}{|A|}\sum_j p(f_i|f_j,T_i,T_j) \quad (4)$$

We minimize the entropy as our objective function, arriving at a set of transformations T.

$$T = \arg\min_T H(f|A,T) = \arg\min_T \left(-\frac{1}{|A|}\sum_i log \frac{1}{|A|}\sum_j \frac{1}{Z} e^{-\frac{D^2(f_i(T_i),f_j(T_j))}{\sigma^2}}\right) \quad (5)$$

Note that to simplify the concept and the notation above, we have not mentioned the fact that the fibers come from several brains. This is implicitly handled in that the transformation T_i applied to fiber f_i is the same transformation that is also applied to all other fibers from that brain. We assume that Z is constant for a given value of σ, and thus does not contribute to the optimization.

2.2 Fiber representation and distance function

For simplicity and computational speed, we convert the input variable-length fiber trajectories to a fixed-length representation (as also proposed by [12, 14]). In practice, representing each fiber by 5 points (endpoints, midpoint, and two intermediate points) was empirically found to be effective for registration.

Using this fiber parameterization, we propose a pairwise fiber distance metric D that is related to the Hausdorff distance (the maximum of the minimum distances between pairs of closest points). We calculate D as the maximum distance between pairs of corresponding points along the fibers (i.e. the first through fifth point pairs). This fiber distance computation can thus take advantage of matrix subtractions. D is a symmetric distance that is the same between fibers (f_i, f_j) and (f_j, f_i), eliminating the issue of the classic Hausdorff measure being a directed distance. Because point ordering along the fiber is not known a priori (a fiber parameterization can equivalently start from either end), D is computed with both possible orderings and the minimum is chosen.

In practice, this method works very well with relatively nearby and corresponding fibers. For more distant fibers the point correspondence and distance measure may not be informative, a known problem with all such fiber distance metrics that have been shown to capture the local structure but poorly reflect the "true relationship" of distant fibers [16]. Luckily in our case, these uninformative large distance measures are unimportant for registration. These far-away, dissimilar, or outlier fibers are distant relative to the radius of interest defined by σ and have little effect on the objective function.

2.3 Implementation

We have implemented a full affine registration framework using a coordinate descent method. The code is a Python package that uses VTK [7], scipy [5], and numpy [5]. For optimization we use Powell's simplex-based COBYLA (Constrained Optimization by Linear Approximation) method [13] in the scipy.optimize toolkit. The affine parameters are constrained (across subjects) as in other entropy-based congealing methods [8, 20] to avoid an unnecessary overall rotation or translation of all brains, and to avoid the shrink to a point solution that artifactually reduces entropy. We require that all translation, rotation, and shear components sum to 0 over all transforms applied to the data, and that all scale factors average to 1. The COBYLA package allows definition of expected initial step sizes ρ_{beg}, and determines convergence when final step sizes ρ_{end} are under a user-provided threshold, thus we have set these ρ parameters empirically using the expected magnitudes of our transform parameters.

The σ parameter of the Gaussian kernel (eq. 1) has been tuned to enable multi-scale registration. In practice, we run several iterations of optimization, alternating translation and rotation, with an initial σ of 30mm. Next, we decrease σ to 10mm, then to 5mm, and optimize while alternating translation, rotation, scale, and shear. The computation of the

fiber distances has been implemented in a multiprocessor framework. The distances are computed between a random sample of fibers from each input subject (typically 200–300), and another, smaller random sample of these fibers whose size we increase during the registration process (typically beginning with 25 or more fibers). The smaller random sample is resampled (all sampling is done without replacement) each time we change the parameters being optimized. The style of randomly sampling data points at which to compute the objective function has been successfully employed in many registration strategies [11, 8, 20] and in fiber clustering [15]. The terms in eq. 5 that result from comparing fibers from the same brain are neglected.

2.4 Data and processing

N=26 healthy subjects dataset: Diffusion weighted images (DWI) scans were acquired on a 3-T GE system using an echo planar imaging sequence and the following parameters: 51 gradient directions with b=900, eight baseline scans with b=0, TR 17000 ms, TE 78 ms, FOV 24 cm, 144×144 encoding steps, 1.7 mm slice thickness. Artifacts due to eddy currents and head motion were removed by affine registration of diffusion to baseline images using FSL's linear image registration tool (FLIRT). Single-tensor streamline tractography was seeded in the entire brain of each subject in voxels with anisotropy (linear measure) > 0.2.

3 Results

We performed three registration experiments: objective function probing, synthetic data validation, and multi-subject registration.

Experiment 1: objective function probing

We investigated the behavior of the multi-scale objective function under simple rotation, translation, scaling, and shear. One healthy control subject was chosen, and 2000 trajectories were randomly sampled without replacement, twice, to generate different fixed and moving brains. A range of transformations was applied to the moving brain, and the objective function was computed using all fibers from both brains (see fig. 1). Importantly, results demonstrate that the objective function is very smooth, and that decreasing σ has the desired behavior of increasing sensitivity to small transformations.

Experiment 2: synthetic data validation

Using as input one healthy control subject, we generated synthetic data as follows: 300 trajectories of length greater than 40mm were randomly sampled from the input dataset, and a randomly generated transformation was applied to these trajectories, to generate a "synthetic brain." The parameters of the random transform were: translation up to ±20mm along each axis, scale factor from 0.85 to 1.15 in each axis, and rotation up to ±20 degrees around each axis. To enable unambiguous computation of errors in the other parameters, shear was not included. This procedure was repeated 10 times to generate a dataset of 10 synthetic brains with known ground-truth transformations. The registration pipeline was applied to the 10 brain dataset (see fig. 2), using three levels of scale: σ of 30, 10, and 5mm; and 3 levels of randomly sampled subset fibers: 25, 50, and 75 fibers. These parameters were set empirically as a compromise between fast optimization and good convergence. Errors in the resulting parameters were measured by comparison to the ground truth applied transforms. The mean absolute errors and their standard deviations in each component were: 1.33 ±1.49, 1.50 ±1.20, 2.06 ±2.06 degrees rotation; 0.62 ± 0.456, 0.74 ± 0.548, 2.07 ± 0.770 mm translation; and 0.015 ± 0.014, 0.006 ± 0.007, 0.017 ± 0.015 scale factor magnitude. The method cannot recover any mean transformation that may have been applied (e.g. if all input brains were rotated together by 30 degrees that could not be detected) so any mean transformations were removed from the ground truth transforms before calculation of

the errors. The experiment ran for 48.8 minutes, spending the following amount of time at each level of scale: 6.6 minutes at 30mm, 18.1 minutes at 10mm, and 24 minutes at 5mm. (The computing environment was a 2x2.26 GHz Quad-Core Mac with 16GB of memory. Note that reported run times could be improved by coding in C rather than python, and/or increasing use of multiprocessing, however this initial implementation is a proof of concept.)

Experiment 3: multi-subject dataset

The proposed registration method was applied to the full (N=26) healthy control multi-subject dataset (see fig. 3). The registration pipeline used 200 randomly sampled fibers of length greater than 60mm per subject, three levels of scale: σ of 30, 10, and 5mm; and 4 levels of numbers of randomly sampled subset fibers: 25, 50, 75, and 100 fibers. The method spent 48 minutes at the 30mm scale, 188 minutes at the 10mm scale, and 235 minutes at the 5mm scale. The results demonstrate successful alignment of the brains, as can be appreciated visually in fig. 3, where the output trajectories look locally similar and parallel, and the subject colors are generally mixed locally (i.e. trajectories from many subjects are neighboring).

4 Discussion and Conclusion

We have proposed a probabilistic atlas model for tractography that enables the computation of the entropy of a collection of fibers, and we have shown that registration by minimizing this entropy can successfully align the white matter in multiple subjects. Advantages of our objective function include its smoothness and the fact that any fiber outliers will have little effect. Optimization of the proposed objective, because it is based on tractography data, has the potential to enhance downstream tractography modeling and statistical analysis results. Future work will include code optimization, incorporation of higher-order deformations, and comparison of the method to other fiber- and image-based registration methods. To our knowledge, this work represents the first method for groupwise registration of whole-brain diffusion tractography data.

Acknowledgments

We gratefully acknowledge support from NIH grants R21CA156943, P41RR019703, R01MH074794, R01MH092862, P41RR013218 and P41EB015902, and CIMIT.

References

1. Caan M, Majoie C, van Vliet L, van der Graaff M, Vos F. Non-rigid point set matching of white matter tracts for diffusion tensor image analysis. Biomedical Engineering, IEEE Transactions on. 2010; 58(9):2431– 2440.
2. Corouge I, Fletcher P, Joshi S, Gouttard S, Gerig G. Fiber tract-oriented statistics for quantitative diffusion tensor MRI analysis. Medical Image Analysis. 2006; 10(5):786–798. [PubMed: 16926104]
3. Durrleman S, Fillard P, Pennec X, Trouvé A, Ayache N. Registration, atlas estimation and variability analysis of white matter fiber bundles modeled as currents. NeuroImage. 2011; 55:1073–1090. [PubMed: 21126594]
4. Goodlett C, Fletcher P, Gilmore J, Gerig G. Group analysis of DTI fiber tract statistics with application to neurodevelopment. NeuroImage. 2009; 45(1):133–142.
5. Jones, E.; Oliphant, T.; Peterson, P., et al. SciPy: Open source scientific tools for Python (2001–). http://www.scipy.org/
6. Joshi S, Davis B, Jomier M, Gerig G. Unbiased diffeomorphic atlas construction for computational anatomy. NeuroImage. 2004; 23:151–160.

7. Kitware: VTK: The Visualization Toolkit. http://www.vtk.org/
8. Learned-Miller E. Data driven image models through continuous joint alignment. Pattern Analysis and Machine Intelligence, IEEE Transactions on. 2006; 28(2):236–250.
9. Leemans A, Sijbers J, De Backer S, Vandervliet E, Parizel P. Multiscale white matter fiber tract coregistration: A new feature-based approach to align diffusion tensor data. Magnetic Resonance in Medicine. 2006; 55(6):1414–1423. [PubMed: 16685732]
10. Maddah M, Grimson W, Warfield S, Wells W. A unified framework for clustering and quantitative analysis of white matter fiber tracts. Medical Image Analysis. 2008; 12(2):191–202. [PubMed: 18180197]
11. Mattes D, Haynor D, Vesselle H, Lewellen T, Eubank W. PET-CT image registration in the chest using free-form deformations. Medical Imaging, IEEE Transactions on. 2003; 22(1):120–128.
12. Mayer A, Zimmerman-Moreno G, Shadmi R, Batikoff A, Greenspan H. A supervised framework for the registration and segmentation of white matter fiber tracts. Medical Imaging, IEEE Transactions on. 2011; 30(1):131–145.
13. MJD, P. A direct search optimization method that models the objective and constraint functions by linear interpolation. Kluwer Academic; Dordrecht: 1994. Advances in Optimization and Numerical Analysis, chap; p. 51-67.
14. O'Donnell L, Rigolo L, Norton I, Westin CF, Golby A. fMRI-DTI modeling via landmark distance atlases for prediction and detection of fiber tracts. NeuroImage. 2011
15. O'Donnell L, Westin CF. Automatic tractography segmentation using a high-dimensional white matter atlas. Medical Imaging, IEEE Transactions on. 2007; 26(11):1562–1575.
16. Tsai, A.; Westin, CF.; Hero, A.; Willsky, A. Computer Vision and Pattern Recognition. IEEE; 2007. Fiber tract clustering on manifolds with dual rooted-graphs; p. 1-6.
17. Wassermann, D.; Rathi, Y.; Bouix, S.; Kubicki, M.; Kikinis, R.; Shenton, M.; Westin, CF. Information Processing in Medical Imaging. Springer; 2011. White matter bundle registration and population analysis based on gaussian processes; p. 320-332.
18. Zhang H, Avants B, Yushkevich P, Woo J, Wang S, McCluskey L, Elman L, Melhem E, Gee J. High-dimensional spatial normalization of diffusion tensor images improves the detection of white matter differences: an example study using amyotrophic lateral sclerosis. Medical Imaging, IEEE Transactions on. 2007; 26(11):1585–1597.
19. Ziyan U, Sabuncu M, Grimson W, Westin CF. Consistency clustering: A robust algorithm for group-wise registration, segmentation and automatic atlas construction in diffusion MRI. Int J Comput Vis. 2009; 85(3):279–290. [PubMed: 20442792]
20. Zöllei L, Learned-Miller E, Grimson E, Wells W. Efficient population registration of 3D data. Computer Vision for Biomedical Image Applications. 2005:291–301.
21. Zvitia O, Mayer A, Shadmi R, Miron S, Greenspan H. Co-registration of white matter tractographies by adaptive-mean-shift and gaussian mixture modeling. Medical Imaging, IEEE Transactions on. 2010; 29(1):132–145.

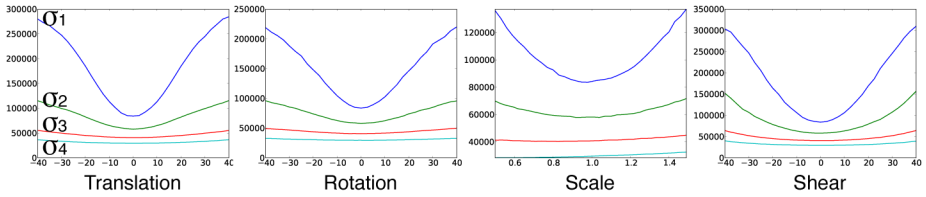

Fig. 1.

Plots of the objective function under x-translation (−40 to 40mm), rotation about x (−40 to 40 degrees), scaling along x (factors of 0.5 to 1.5), and shear (−40 to 40 degrees skew about x). The curves represent different values of the multi-scale parameter σ: 5mm (top curve, blue), 10mm, 20mm, and 30mm (lowest curve, cyan).

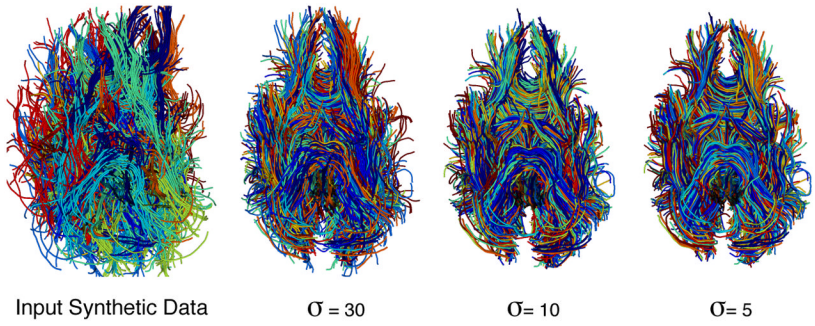

Fig. 2.

Results of multi-scale registration of randomly transformed synthetic brain (n=10) dataset (inferior view). Each subject is shown in a different color. The output brains are shown after each registration scale (σ), demonstrating successful coarse-to-fine registration. The output brains appear slightly "rotated" relative to standard AC-PC orientation due to some mean component of the initial random transforms.

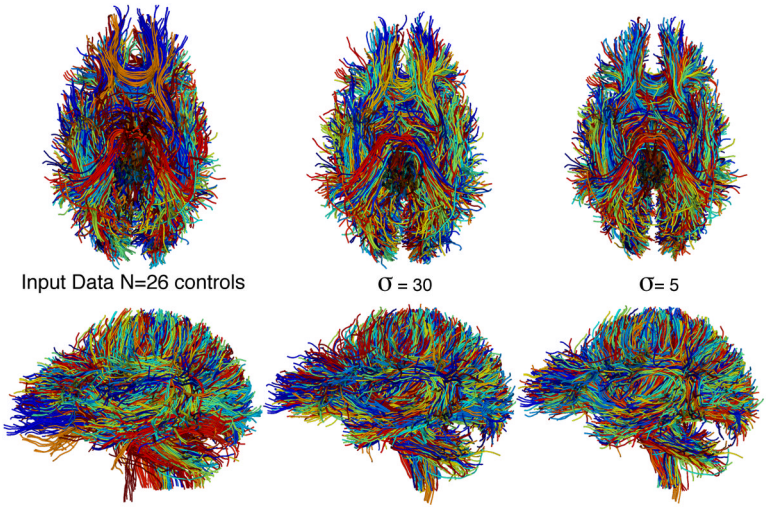

Fig. 3.
Results in N=26 healthy subject dataset demonstrate successful coarse-to-fine registration (inferior and left views shown). Each subject is shown in a different color.